

## Size-Dependent High-order Harmonic Generation in Rare-Gas Clusters

Hyunwook Park,\* Zhou Wang, Hui Xiong, Stephen B. Schoun, Junliang Xu, Pierre Agostini, and Louis F. DiMauro  
*Department of Physics, The Ohio State University, Columbus, Ohio 43210, USA*

(Received 28 August 2014; published 31 December 2014)

High-order harmonic generation (HHG) is investigated in rare-gas clusters as a function of the cluster size using 0.8 and 1.3  $\mu\text{m}$  femtosecond lasers. A characteristic, species-dependent knee structure in the single particle response is observed. A 1D recollision model qualitatively reproduces this behavior and associates it to the degree of delocalization of the initial wave function. Small clusters are observed to have a higher efficiency than monomers but rapidly lose this advantage as the size increases. The implications of these findings on the HHG mechanism in clusters are discussed.

DOI: 10.1103/PhysRevLett.113.263401

PACS numbers: 36.40.-c, 42.65.Ky, 61.48.-c

High-order harmonic generation (HHG) resulting from the interaction of a high intensity laser with free atoms is well described by the single-active electron, rescattering quantum model [1]. Alternatively, in solids the HHG characteristics suggest a different mechanism based on field-driven Bloch oscillations [2,3]. Over the past 25 years, HHG from noble gases has become a practical source of femtosecond and attosecond XUV radiation [4–7]. Despite several efforts over this period, the poor conversion efficiency,  $10^{-8} - 10^{-5}$ , remains problematic [8]. In this context, van der Waals (vdW) clusters, among other systems, have been examined as a potential HHG medium [9,10].

vdW clusters are attractive systems since they combine the low average density of gases and the local high density of solids. vdW clusters are easily produced in supersonic expansion of inert gas atoms, and the size distribution, although broad, is controllable by the backing pressure and reservoir temperature [11,12]. The mechanism underlying HHG in clusters is not totally identified. Numerical solutions of the time-dependent Schrödinger equation have suggested that the cutoff energy could be dramatically extended in clusters due to tunnel ionization by one atom and recombination to another through Bremsstrahlung incoherent emission [13,14]. A prior study [15] did report an increase in the cluster cutoff energy, although it was much smaller than the predicted  $I_p + 8U_p$  (6 eV compared to 60 eV) and even smaller than the simple molecular effect [16]. In addition, the question of the yield is still open since extracting the single particle response is always challenged by the macroscopic aspect, i.e., phase matching. Tisch *et al.* [10] have observed that the harmonic yield in xenon clusters increases more rapidly with backing pressure than atoms, but the role of the phase matching was not addressed. Vozzi *et al.* [15] have measured the yield of argon clusters versus temperature near the atomic ionization saturation intensity and found that, for sizes larger than 7000 atoms, the HHG is limited to the cluster surface. Ruf *et al.* [17] have concluded, by measuring the ellipticity dependence, that HHG in clusters is a recollision process, a

conclusion far from intuitive since one of the main features of vdW clusters interaction with lasers is the occurrence of “inner ionization” [18], i.e., the appearance of quasifree electrons which can move around but are still inside the cluster.

In this Letter we investigate the cluster HHG as a function of both backing pressure and temperature for different inert gases and isolate the size signature for the single particle response: a fast increase in the yield up to an optimum size, e.g., 700 atoms for argon, followed by a decreased rate for larger sizes. Using the rescattering model with a delocalized ground state wave function we can qualitatively account for this observation and its dependence on the atomic number,  $Z$  from neon to xenon. In addition, we compare the group delay measured using the RABBITT method [19,20] for clusters and atoms and find additional support of the rescattering model. We also directly compare the harmonic yields of pure monomers and clusters at the same atomic density. After identifying the phase-matching contribution, we show that the single particle emission in clusters is more efficient than the atom but only over a restricted cluster size. We also observe no evidence of a change in the cutoff energy for clusters and atoms.

One initial question about HHG from clusters is whether the structure remains intact during the laser pulse. At high intensity, the dynamics of the cluster is driven by the ionization, initially by the laser and later by hot electron impact [21]. As electrons leave the cluster, a net positive charge develops, the ions repel each other, and eventually the cluster disintegrates. For intensities  $\geq 10^{15} \text{ W/cm}^2$ , argon clusters appear to structurally evolve in a few femtoseconds [22]. As the intensity is lowered, ionization is reduced, slowing down the cluster’s disassembly. In our experimental conditions, the total ionized fraction per cluster does not exceed 2% [23]. Consequently, the cluster expansion is slowed down to a few hundred femtoseconds, as estimated by an expanding fluid-sphere model [21]. Thus we assume that the HHG emission originates from

stable cluster structures on the 30–65 fs time scale of our laser pulses.

To facilitate a direct comparison between clusters and monomers, a solenoid valve (Even-Lavie, ATAD Inc.) [24] and a homemade continuous-gas nozzle are mounted on a three-axis translation stage such that both are located at the same position along the optical propagation axis but 2 cm apart in the transverse direction. This configuration allows monomer and cluster to experience the same laser intensity and Gouy phase, and also allows rapid switching between sources. The clusters are produced by adiabatic gas expansion from a trumpet shaped nozzle with an exit diameter of 150  $\mu\text{m}$ . The backing pressure is regulated with 10 mbar precision and the valve temperature can be varied from 100–400 K with  $\pm 0.2$  K stability. A Ti: sapphire amplifier system (Femtolaser GmbH, model FemtoPower) centered at 790 nm generates 30 fs, 0.5 mJ pulses at a 3-kHz-repetition rate. The pulse is focused in front of the gas jet producing an intensity  $\sim 10^{14}$  W/cm<sup>2</sup>. A 150  $\mu\text{m}$ -thick Al filter suppresses the fundamental light before the XUV spectrometer. The XUV spectrometer (Hettrick SXR-II) uses a Kirkpatrick-Baez mirror pair geometry and a back-illuminated charge-coupled-device camera (Andor DO440). The RABBITT group delay measurements are performed in a separate harmonic apparatus (see Schoun *et al.* for details [25]). For the RABBITT experiment, 65 fs, 1.3  $\mu\text{m}$  pulses, which produce a higher cutoff energy and a finer frequency comb, are produced by a commercial optical parametric amplifier (HE-TOPAS, Light Conversion) and focused 4 mm before the jet with an intensity of  $1.2 \times 10^{14}$  W/cm<sup>2</sup>. The RABBITT detection gas is neon since its XUV photoionization cross section is relatively uniform and featureless over the energy range of interest. Both experiments are optimized for short trajectory phase matching, while the long trajectory contributions are minimized by an on-axis pinhole.

We first discuss the relative efficiency of clusters and monomers. Figure 1 compares the 31st-order harmonic yield measured at the wavelength of 0.8  $\mu\text{m}$  at room temperature (the harmonic yield averaged over orders 19 to 35 gives a similar result). For comparison of the yields, the backing pressure is converted into the atomic density  $n_0$  in the interaction region by measuring diameters of the cluster and monomer jets. The jet diameter is obtained by measuring the harmonic signal along the transverse direction of the jet propagation axis. Our density estimate agrees well with simulated results [11,24] and measurements of Luria *et al.* [24]. The monomer's harmonic yield in Fig. 1 follows a quadratic law below  $3 \times 10^{17}$  cm<sup>-3</sup>. A faster growth is observed at higher density as the phase matching approaches the maximum coherence length; this behavior is reproduced in the calculated yield curve [26]. For clusters, the harmonic yield initially increases rapidly, i.e.,  $n_0^5$ , and is larger than the monomer's. The harmonic

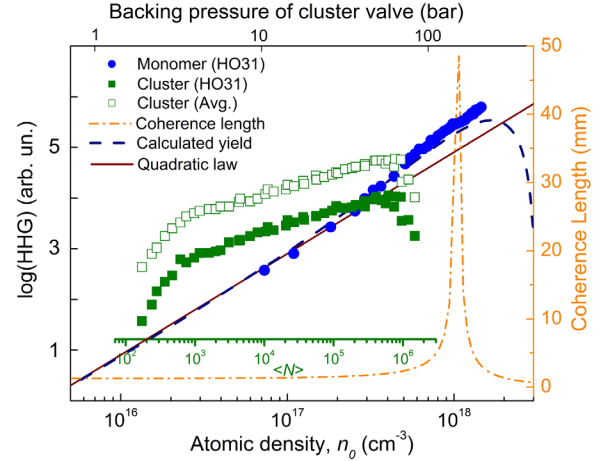


FIG. 1 (color online). Comparison of harmonic yields of the argon monomer (blue circles) and cluster (green squares) as a function of atomic density measured in the XUV spectrometer. The average yield (green open squares) of the cluster is shifted for clarity. The backing pressure of the cluster valve is given on the top abscissa and the mean cluster size is given with the color-matching (green) scale. The quadratic law (brown solid line), calculated yield (navy dashed line), and coherence length (orange-dashed dotted line) are presented for comparison. The scale of the coherence length is given on the right axis.

emission then slows down above  $n_0 \approx 2 \times 10^{16}$  cm<sup>-3</sup>, i.e., an average size of  $\langle N \rangle = 700$  [11]). The rapid drop beyond the density of  $4 \times 10^{17}$  cm<sup>-3</sup> is caused by the backing pressure approaching the maximum valve operation (100 bar). However, the results clearly show that clusters are more efficient harmonic generators up to  $n_0 \sim 3 \times 10^{17}$  cm<sup>-3</sup> and beyond this density the monomer catches and exceeds in yield.

Second, we show in Fig. 2(a) the RABBITT measurement of the argon group delay (GD) at 1.3  $\mu\text{m}$  for the monomer and clusters and compare this to the classical prediction for the attochirp. The calculated attochirp agrees with the measurements except near the Cooper minimum ( $\sim 50$  eV), as expected (see [25]). The positive slope of the attochirp, e.g., positive dispersion, arises from the preferential phase matching of short trajectories for our geometry. Remarkably, the cluster and monomer GD show a striking similarity suggesting that the mechanism for high harmonic generation is the same, the three-step rescattering model rather than the Bloch model [2]. Our result is consistent with the ellipticity study by Ruf *et al.* [17].

Last, our comparative study addresses the question of the harmonic energy cutoff. Using photoelectron spectroscopy, the high harmonic distribution driven by 1.3  $\mu\text{m}$  pulses is shown in Fig. 2(b). The cluster and monomer distributions are recorded by filtering the HHG comb either through an Al or Zr thin film. The Al and Zr transmission complement each other and cover the entire range of interest (20 to 120 eV). The intensity of 1.3  $\mu\text{m}$  ( $1.2 \times 10^{14}$  W/cm<sup>2</sup>) corresponds to a cutoff beyond the Cooper minimum

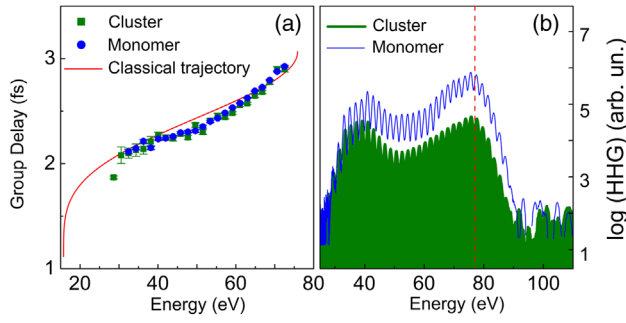


FIG. 2 (color online). Comparisons of the argon monomer and cluster ( $\langle N \rangle = 10^5$ ) HHG distributions measured with our RABBITT apparatus. (a) Group delay for monomer (blue circles) and cluster (green squares) and the solid red line is the classical attochirp for short trajectories. (b) Harmonic distribution for the monomer (blue curve) and cluster (green-shaded area), respectively.

region which makes the cutoff measurement more accurate. Overall, the distribution of the cluster appears identical to the monomer excluding some minor differences. Most importantly, the energy cutoff  $E_c$  is the same as indicated by the red-dotted line. The observed cutoff is also consistent with the classical cutoff prediction of  $E_c = I_p + 3.2U_p = 77$  eV [27], where the intensity is independently determined by the RABBITT GD measurement. This result suggests that the recombination dipole in inert gas clusters resulting in coherent emission occurs on its parent ion and not neighboring sites as suggested in [13,14]. Note, our experiment may not have the sensitivity to observe this incoherent emission.

From a fundamental perspective, it is interesting to isolate the size effect of a *single* cluster, i.e., to bridge the gap between the single atom and the solid state [28]. However, HHG is detected as the coherent emission of an ensemble of individual emitters, and, thus, phase matching can mask the microscopic behavior. In this work, we are able to disentangle the microscopic and macroscopic contributions by controlling both the backing pressure ( $p_b$ ) and the nozzle temperature ( $T_n$ ) of the cluster source, enabling extraction of the cluster size effect. When the nozzle temperature and the backing pressure are varied,  $T_n = 153$ – $373$  K and  $p_b = 0.5$ – $7$  bar, the mean cluster size  $\langle N \rangle$ , i.e., the average number of atoms per cluster determined by the Hagen relation [11], and the cluster density vary.

The harmonic yield versus the atomic density  $n_0 \propto p_b/kT_n$  shows a characteristic behavior displayed in Fig. 3(b) with a break point, or knee, which depends on the temperature, indicated by the vertical dashed lines. This suggests that the knee is not a phase-matching effect since the optimal coherence length would occur at the same density. In addition, when the harmonic yield per cluster is plotted against the cluster size in Fig. 3(a), the curves coincide and the knee is independent of the choice of

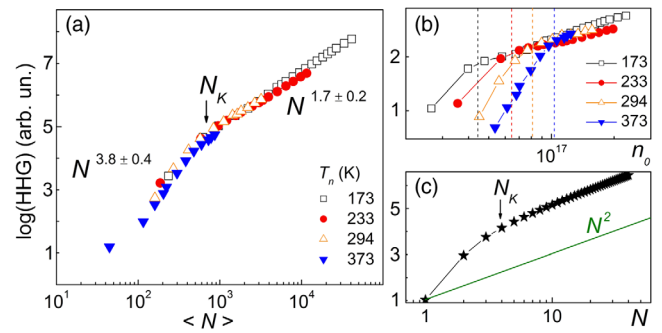


FIG. 3 (color online). The log scale of the 21st-order harmonic yields (the average of orders 19–31 gave a similar result),  $\log(\text{HHG})$ , in argon clusters. (a) and (b) The measurements of  $\log(\text{HHG})$  from the XUV spectrometer plotted as functions of  $\langle N \rangle$  (atoms per cluster) and relative atomic density,  $n_0$  ( $\text{cm}^{-3}$ ), respectively. Only four temperature curves are shown—note that the scale of the gas pressure is different for each curve. (c) The calculation of  $\log(\text{HHG})$  as a function of the cluster size  $N$ .

( $p_b$ ,  $T_n$ ). The harmonic yield for an isolated cluster is obtained by dividing the yield (at certain  $p_b$  and  $T_n$ ) by the square of the cluster density. From this we conclude that the observed behavior is the response of a single cluster particle. Additional evidence is that the occurrence of the knee is below the peak density needed for the optimal coherence length and the observed growth is not amenable to the calculation [26] which well describes the monomer behavior shown in Fig. 1.

We find that two factors can contribute to a yield increase faster than  $N^2$ . (i) Enhanced ionization: the cluster ionization energy depends on the cluster size [28], which, according to tunneling theory [23], results in an increase in the ionization rate. This effect is, however, small. (ii) Partial delocalization of electron wave function (EWF): this is a more significant factor since it directly affects the dipole resulting in a larger polarizability. A classical calculation of polarizability in clusters shows a size-dependent enhancement effect [29], but it is not clear how it affects HHG [30,31]. If delocalization were to simply follow the increase of the size, i.e., be proportional to  $N$ , the yield increase rate would be constant. The crucial finding of our experiment is the existence of a knee at a critical size  $N_K$  that separates the  $N^{3.8 \pm 0.4}$  from the  $N^{1.7 \pm 0.2}$  rates, implying that delocalization increases up to  $N_K$  only and remains constant beyond that point.

In order to investigate this we implemented the Lewenstein's quantum rescattering model with a 1D Coulomb potential for the parent ion at the position ( $x_i$ ) and  $N - 1$  Yukawa potentials for the other neutral atoms ( $x_{j \neq i}$ ). The model entails a solution of the time-independent Schrödinger equation partially delocalized over only the nearest neighbors and quickly becomes independent of  $N$ . In practice, we have chosen soft-core potentials to describe the parent ion and all other neutrals,

$$V(N, x) = \frac{-1}{\sqrt{(x - x_i)^2 + a_{\text{ion}}}} + \sum_{j \neq i}^N \frac{-e^{-|x-x_j|/b}}{\sqrt{(x - x_j)^2 + a_{\text{neut}}}}, \quad (1)$$

where  $a_{\text{ion}}$ ,  $a_{\text{neut}}$ , and  $b$  are parameters determined based on the electron localization probability within the atomic radius  $r_{np}$  (where  $n = 2, 3, 4$ , and  $5$  for Ne, Ar, Kr, and Xe, respectively) [32]. Note that a similar idea has been used in other cluster simulations [13,33,34]. The choice of these parameters determines the delocalization, which, albeit small in vdW clusters, reflects the EWF extension to its neighbor atoms due to the tightly packed structure [30,32,35]. The time dependent dipole as a function of the cluster size is then calculated using the Lewenstein model with the saddle point approximation [1]. The EWF delocalization has the consequence of increasing the dipole amplitude, thus resulting in a more rapid growth of the harmonic yield. For very small sizes the EWF occupies essentially the whole cluster but as the number of atoms grows beyond a certain limit, the delocalization and hence the dipole does not further increase and the cluster behaves as an ensemble of independent atoms.

Figure 3(c) shows that the result of the calculation for argon clusters qualitatively agrees with the size-dependent behavior observed in the experimental HHG yield shown in Fig. 3(a). The delocalized-modified ground-state EWF plays the essential role in enhancing the growth rate for HHG emission in the Lewenstein model. For comparison, a perfectly localized EWF results in a quadratic growth in the HHG yield with the cluster size, as shown by the green-solid line in Fig. 3(c), similar to the monomer gas behavior with atomic density shown in Fig. 1. Note that field screening and XUV reabsorption (within the cluster) effects, which presumably causes the growth rate of  $N^{1.7(<2)}$  (less than quadratic), are not included in the model. Clearly, the knee transition in the 1D model occurs with fewer atoms as compared to the experiment, e.g.,  $N_K = 4$  versus 700 argon atoms. However, for a meaningful comparison, one must extrapolate the calculation into three dimensions: adding two atoms in the 1D model equates to adding one shell in three dimensions. Thus 700 atoms in three dimensions corresponds only to a 5-layer icosahedral cluster [36], i.e., to 10 neighbors in one dimension. The model successfully predicts a species dependence of the knee, directly related to the amount of initial delocalization, as measured by the atomic radius relative to the interatomic distance [30,32,35]: the more compact the cluster, the stronger the delocalization. Actually a tighter structure is a consequence of a stronger delocalization of electrons as observed in the experiment (Table I).

The agreement, albeit qualitative, between the model and the experiment, as well as the group delay and the cutoff measurements, support the validity of the recollision model

TABLE I. Species dependent knee point  $N_K$  with its layer size  $N_{\text{shell}}$  which indicates the number of atomic layers for an  $N_K$ -size cluster [36].

	Ne	Ar	Kr	Xe
$N_K$ (Exp)	150	700	1100	1900
$N_{\text{shell}}$ (Exp)	3	5	6	7
$N_{\text{shell}}$ (Mod)	1	2	3	4

as the mechanism for HHG in inert gas clusters. The calculated harmonic distributions from the model do not show a cutoff energy extension—as Lewenstein’s model includes only recombination with the parent ion, in agreement with the observation. It results from the above considerations that, perhaps surprisingly, the three-step model is applicable to a cluster with several hundreds or even thousands of atoms, which nevertheless does not quite behave as an ensemble of independent atoms because the partial delocalization of the initial wave function, which plays a key role, is a characteristic property of the cluster. The delocalization can be estimated to extend over a few atomic layers. The absence of cutoff extension is consistent with the model whose conclusions are restricted to the moderate to low laser intensity. A high degree of ionization rate would certainly invalidate the single-active electron model.

In conclusion, the high-order harmonic generation in rare-gas clusters shows a universal dependence on the size that is interpreted by a single-active-electron 1D cluster model with a partially delocalized electron wave function based on the three-step model of Lewenstein’s quantum calculation. This is to be compared to a similar conclusion drawn from HHG in big molecules like  $C_{60}$  for which the recollision model was also found to agree with experiment [37]. From a practical point of view, although the enhancement of the harmonic yield is observed (in a limited range of the size), the clusters cannot compete with the monomers as a medium for applications.

This work is supported by the Army Research Office (W911NF-11-1-0120), the Air Force Office of Scientific Research (FA9550-12-1-0047), and the NSF. The authors gratefully acknowledge helpful discussions with Dr. J. Marangos and Dr. F. Catoire. L. F. D. acknowledges support from the Hagenlocker chair.

\*park.1771@osu.edu

- [1] M. Lewenstein, P. Balcou, M. Y. Ivanov, A. L’Huillier, and P. B. Corkum, *Phys. Rev. A* **49**, 2117 (1994).
- [2] S. Ghimire, A. D. DiChiara, E. Sistrunk, P. Agostini, L. F. DiMauro, and D. A. Reis, *Nat. Phys.* **7**, 138 (2011).
- [3] O. Schubert, M. Hohenleutner, F. Langer, B. Urbanek, C. Lange, U. Huttner, D. Golde, T. Meier, M. Kira, S. W. Koch, and R. Huber, *Nat. Photonics* **8**, 119 (2014).

- [4] P. H. Bucksbaum, *Science* **317**, 766 (2007).
- [5] C. Altucci, R. Velotta, and J. Marangos, *J. Mod. Opt.* **57**, 916 (2010).
- [6] F. Krausz and M. Ivanov, *Rev. Mod. Phys.* **81**, 163 (2009).
- [7] A. L'Huillier, D. Descamps, A. Johansson, J. Norin, J. Mauritsson, and C.-G. Wahlström, *Eur. Phys. J. D* **26**, 91 (2003).
- [8] T. Brabec and F. Krausz, *Rev. Mod. Phys.* **72**, 545 (2000).
- [9] T. D. Donnelly, T. Ditmire, K. Neuman, M. D. Perry, and R. W. Falcone, *Phys. Rev. Lett.* **76**, 2472 (1996).
- [10] J. Tisch, T. Ditmire, D. J. Fraser, N. Hay, M. B. Mason, E. Springate, J. P. Marangos, and M. H. R. Hutchinson, *J. Phys. B* **30**, L709 (1997).
- [11] O. F. Hagen, *Rev. Sci. Instrum.* **63**, 2374 (1992).
- [12] K. J. Mendham, N. Hay, M. B. Mason, J. W. G. Tisch, and J. P. Marangos, *Phys. Rev. A* **64**, 055201 (2001).
- [13] J. V. de Aldana and L. Roso, *J. Opt. Soc. Am. B* **18**, 325 (2001).
- [14] D. F. Zaretsky, P. Korneev, and W. Becker, *J. Phys. B* **43**, 105402 (2010).
- [15] C. Vozzi, M. Nisoli, J.-P. Caumes, G. Sansone, S. Stagira, S. De Silvestri, M. Vecchiocattivi, D. Bassi, M. Pascolini, L. Poletto, P. Villoresi, and G. Tondello, *Appl. Phys. Lett.* **86**, 111121 (2005).
- [16] A. D. Bandrauk and H. Yu, *J. Phys. B* **31**, 4243 (1998).
- [17] H. Ruf, C. Handschin, R. Cireasa, N. Thiré, A. Ferré, S. Petit, D. Descamps, E. Mével, E. Constant, V. Blanchet, B. Fabre, and Y. Mairesse, *Phys. Rev. Lett.* **110**, 083902 (2013).
- [18] U. Saalmann, *J. Mod. Opt.* **53**, 173 (2006).
- [19] P. M. Paul, E. S. Toma, P. Breger, G. Mullot, F. Aue, P. Balcou, H. G. Muller, and P. Agostini, *Science* **292**, 1689 (2001).
- [20] H. Muller, *Appl. Phys. B* **74**, s17 (2002).
- [21] T. Ditmire, T. Donnelly, A. M. Rubenchik, R. W. Falcone, and M. D. Perry, *Phys. Rev. A* **53**, 3379 (1996).
- [22] E. Skopalová, Y. C. El-Taha, A. Zair, M. Hohenberger, E. Springate, J. W. G. Tisch, R. A. Smith, and J. P. Marangos, *Phys. Rev. Lett.* **104**, 203401 (2010).
- [23] M. Ammosov, N. B. Delone, and V. P. Krainov, *Zh. Eksp. Teor. Fiz.* **91**, 2008 (1986) [*Sov. Phys. JETP* **64**, 1191 (1986)].
- [24] K. Luria, W. Christen, and U. Even, *J. Phys. Chem. A* **115**, 7362 (2011).
- [25] S. B. Schoun, R. Chirila, J. Wheeler, C. Roedig, P. Agostini, L. F. DiMauro, K. J. Schafer, and M. B. Gaarde, *Phys. Rev. Lett.* **112**, 153001 (2014).
- [26] S. Kazamias, S. Daboussi, O. Guilbaud, K. Cassou, D. Ros, B. Cros, and G. Maynard, *Phys. Rev. A* **83**, 063405 (2011).
- [27] J. L. Krause, K. J. Schafer, and K. C. Kulander, *Phys. Rev. Lett.* **68**, 3535 (1992).
- [28] J. Jortner, *Z. Phys. D* **24**, 247 (1992).
- [29] H.-Y. Kim, J. O. Sofo, D. Velegol, M. W. Cole, and G. Mukhopadhyay, *Phys. Rev. A* **72**, 053201 (2005).
- [30] R. Feifel, M. Tchapyguine, G. Öhrwall, M. Salonen, M. Lundwall, R. R. T. Marinho, M. Gisselbrecht, S. L. Sorensen, a. Naves de Brito, L. Karlsson, N. Mårtensson, S. Svensson, and O. Björneholm, *Eur. Phys. J. D* **30**, 343 (2004).
- [31] M. Lein, *Phys. Rev. A* **72**, 053816 (2005).
- [32] E. Clementi and D. L. Raimondi, *J. Chem. Phys.* **38**, 2686 (1963).
- [33] V. Vénier, R. Taïeb, and A. Maquet, *Phys. Rev. A* **65**, 013202 (2001).
- [34] S. X. Hu and Z. Z. Xu, *Phys. Rev. A* **56**, 3916 (1997).
- [35] N. Ashcroft and N. Mermin, *Solid State Physics* (Cengage Learning, Boston, 1976), p. 401.
- [36] J. Farges, M. F. de Feraudy, B. Raoult, and G. Torchet, *J. Chem. Phys.* **84**, 3491 (1986).
- [37] V. R. Bhardwaj, P. B. Corkum, and D. M. Rayner, *Phys. Rev. Lett.* **93**, 043001 (2004).